HHS Public Access

Author manuscript

Neurobiol Dis. Author manuscript; available in PMC 2017 November 01.

Published in final edited form as:

Neurobiol Dis. 2016 November ; 95: 194–203. doi:10.1016/j.nbd.2016.07.024.

The ADHD-linked Human Dopamine D4 Receptor Variant D4.7 Induces Over-Suppression of NMDA Receptor Function in Prefrontal Cortex

Luye Qin[1,*], **Wenhua Liu**[1,2,*], **Kaijie Ma**[1], **Jing Wei**[1], **Ping Zhong**[1], **Kei Cho**[3], and **Zhen Yan**[1,#]

[1]Dept. of Physiology & Biophysics, State University of New York at Buffalo, School of Medicine and Biomedical Sciences, Buffalo, NY 14214, USA

[2]School of Life Science, Zhaoqing University, Zhaoqing, 526061 China

[3]The MRC Centre for Synaptic Plasticity, University of Bristol Whitson, Bristol, UK

Abstract

The human dopamine D4 receptor (hD_4R) variants with long tandem repeats in the third intracellular loop have been strongly associated with attention deficit hyperactivity disorder (ADHD) and risk taking behaviors. To understand the potential molecular mechanism underlying the connection, we have investigated the synaptic function of human D_4R polymorphism by virally expressing the ADHD-linked 7-repeat allele, hD4.7, or its normal counterpart, hD4.4, in the prefrontal cortex (PFC) of D_4R knockout mice. We found that hD_4R bound to the SH3 domain of PSD-95 in a state-dependent manner. Activation of hD4.7 caused more reduction of NR1/PSD-95 binding and NR1 surface expression than hD4.4 in PFC slices. Moreover, the NMDAR-mediated excitatory postsynaptic currents (NMDAR-EPSC) in PFC pyramidal neurons were suppressed to a larger extent by hD4.7 than hD4.4 activation. Direct stimulation of NMDARs with the partial agonist D-cycloserine prevented the NMDAR hypofunction induced by hD4.7 activation. Moreover, hD4.7-expressing mice exhibited the increased exploratory and novelty seeking behaviors, mimicking the phenotypic hallmark of human ADHD. D-cycloserine administration ameliorated the ADHD-like behaviors in hD4.7-expressing mice. Our results suggest that over-suppression of NMDAR function may underlie the role of hD4.7 in ADHD, and enhancing NMDAR signaling may be a viable therapeutic strategy to ADHD humans carrying the D4.7 allele.

[#]Correspondence should be addressed to Zhen Yan, Ph.D., Department of Physiology and Biophysics, State University of New York at Buffalo, 124 Sherman Hall, Buffalo, NY, 14214, USA. zhenyan@buffalo.edu.

[*]These authors contributed equally.

Conflict of Interest

None of the authors have a financial interest related to this work.

Introduction

Attention-deficit Hyperactivity disorder (ADHD), a prevalent and debilitating disorder characterized by inattention, hyperactivity, and impulsivity, is highly heritable and multifactorial (Thapar and Cooper, 2015; Hawi et al., 2015). One established candidate gene is the dopamine D4 receptor (Bobb et al., 2005; Grady et al., 2003; Swanson et al., 2007). The gene encoding human D4 receptor (hD4R) uniquely contains a large number of polymorphisms in the coding region for the third intracellular loop, which consists of a variable number (2–11) of 48-bp proline-rich tandem repeats (VNTR, Van Tol et al., 1992). The two most common variants contain 4 and 7 repeats (hD4.4, hD4.7), with the global frequency of 64% and 21%, respectively (Chang et al., 1996). Clinical studies have found a high prevalence of the hD4.7 variant in children diagnosed with ADHD (Grady et al., 2003; Altink et al., 2012; Berry et al., 2013; Trejo et al., 2015), and in people with personality traits of novelty seeking, risk taking, substance abuse and impulsivity (Ebstein et al., 1996; Benjamin et al., 1996; Li et al., 2004; Reiner and Spangler, 2011).

The proline-rich repeats in hD4R provide the binding sites for other proteins containing the SH3 domain. So far the molecular mechanism and functional significance of the remarkable VNTR polymorphism of hD4R is poorly understood. D4 receptors are highly enriched in prefrontal cortex (PFC, Mrzljak et al., 1996; Wedzony et al., 2000; Rubinstein et al., 2001), a brain region subserving high-level “executive” functions, many of which are disrupted in ADHD (Avale et al., 2004; Batty et al., 2015; Yamaguchi et al., 2015). The glutamatergic transmission in PFC plays a key role in determining PFC functions (Goldman-Rakic, 1995; Lisman et al., 1998; Popoli et al., 2011; Yuen et al., 2011; 2012). NMDA-type glutamate receptors are anchored to the synaptic membrane by binding to SH3 domain-containing scaffolding proteins, such as PSD-95 (Roche et al., 2001; Wenthold et al., 2003; Prybylowski et al., 2005). NMDAR dysfunction has been linked to mental disorders including ADHD (Dorval et al., 2007; Jensen et al., 2009; Chang et al., 2014) and autism (Duffney et al., 2015). Our previous studies in rodents have found that D4R activation modulates NMDAR trafficking and function (Wang et al., 2003), and this modulation goes awry in a schizophrenia model (Wang et al., 2006). Administration of methylphenidate (MPH), a dopamine and norepinephrine reuptake inhibitor approved for ADHD treatment, facilitates attention by potentiating PFC NMDAR function (Cheng et al., 2014). These animal studies prompt us to speculate that the ADHD-linked human D4R variants may induce ADHD-like behaviors via dampening NMDAR function through the aberrant interaction with NMDAR/PSD-95 complex.

In the present study, we used D4R knockout mice with viral expression of hD4.4 or hD4.7 in PFC to examine the impact of hD4R polymorphism on NMDARs and ADHD-like behaviors. Our results provide a potential pathophysiological basis for the involvement of human D4R 7-repeat allele in ADHD.

Material and Methods

In vitro Transfection

The HA-tagged human D4.4 and D4.7 plasmids (^{HA}hD4.x) (Rondou et al., 2008) were kindly provided by Dr. Kathleen Van Craenenbroeck at Laboratory of Eukaryotic Gene Expression and Signal Transduction (LEGEST), BELGIUM. HEK293 cells (70%–80% confluent) were transfected with ^{HA}hD4.x (5 μg), Flag-tagged PSD-95 (5 μg, Jo et al., 2010), NR1 (3 μg) and/or NR2B (3 μg) plasmids using Lipofectamine 2000 method.

Generation of hD4.x Viruses

The generation of Sindbis virus used the same procedure as we previously described (Zhong et al., 2015). Briefly, the cDNAs encoding GFP or GFP-hD4.x were subcloned to pSinRep5 vector (Invitrogen) according to the manufacturer's protocol. Recombinant GFP-pSinRep5 or GFP-hD4.x-pSinRep5 was linearized with *Not*I. The DH26S plasmid was linearized using *Xho*I. The linearized templates were transcribed *in vitro* using mMessage Machine SP6 kit (Ambion) and the RNAs were electroporated into baby hamster kidney (BHK) cells. The extracellular medium containing the recombinant viruses was harvested after 24–48 hr. The medium was concentrated on a discontinuous sucrose gradient (55% and 20% sucrose) using ultracentrifugation (160,000× g, 90 min at 4°C).

Animal Surgery

All animal experiments were performed with the approval of the Institutional Animal Care and Use Committee of the State University of New York at Buffalo. *In vivo* virus-based gene delivery into medial PFC was performed as we previously described (Duffney et al., 2015; Zhong et al., 2015). In brief, D4R knockout mice (Rubinstein et al., 1997; 2001, 6–8 weeks) were anesthetized by an i.p. injection of pentobarbital (50 mg/kg), and placed on a stereotaxic apparatus (David Kopf Instruments, Tujunga, CA). The Sindbis viral suspension (1 μl) was injected with a Hamilton syringe (needle gauge 31) at a speed of ~0.2 μl/min. The virus was delivered bilaterally to medial prelimbic area of mice using the following coordinates: 2 mm anterior to bregma; 0.5 mm lateral; and 2 mm dorsal to ventral. Animals were allowed to recover for 1–2 days after viral injection, and analgesia (Carprofen, 5mg/kg, sc) was provided postoperatively during the recovery.

Co-immunoprecipitation

Transfected 293 cells or viral infected brain slices were homogenized in 0.5% NP-40 lysis buffer (0.5% NP-40, 10% glycerol, 50 mM Tris, pH 7.6, 150 mM NaCl, 50mM NaF, 0.1mM EDTA, and 0.1mM Na_3VO_4, 1mM phenylmethylsulfonyl fluoride, and protease inhibitor tablet), then lysates were ultra-centrifuged (200,000 × g) at 4°C for 60 min. Supernatant fractions were incubated with anti-HA (Santa Cruz Biotechnology, sc-805) or anti-NR1 (NeuroMab clone N308/48) for overnight at 4°C, followed by incubation with 50 μl of protein A/G plus agarose (Santa Cruz Biotechnology) for 1 hr at 4°C. Immunoprecipitates were washed three times with lysis buffer containing 0.2 M NaCl, then boiled in 2× SDS loading buffer for 5 min, and separated on 7.5% SDS-polyacrylamide gels. Western blotting experiments were performed with anti-Flag (1:1000, Sigma, F3165), anti-PSD-95 (1:1000,

NeuroMab, 75-028), anti-NR1 (1:500, NeuroMab clone N308/48) or anti-HA (1:200, Santa Cruz Biotechnology, sc-805).

Primary neuronal culture and viral infection

Cortical cultures from D4R knock out mice were prepared. Briefly, frontal cortex was dissected from embryonic day 16 (E16) mouse embryos, and cells were dissociated using trypsin and trituration through a Pasteur pipette. Neurons were plated on coverslips coated with poly-L-lysine in DMEM with 10% fetal calf serum at a density of 1×10^5 cells/cm^2. When neurons were attached to the coverslip within 24 hrs, the medium was changed to Neurobasal with B27 supplement (Invitrogen). Cytosine arabinoside (AraC, 5 μM) was added at DIV3 to stop glial proliferation. Cultured neurons were infected with hD4.4 or hD4.7 Sindbis virus. Electrophysiological recordings were performed on GFP-positive neurons at 2 days after infection.

Electrophysiological recordings

Standard whole-cell voltage-clamp recordings were used to measure synaptic currents in layer V medial PFC pyramidal neurons in brain slices as we described previously (Yuen et al., 2012; Duffney et al., 2015). Two to three days after virus injection, mice were sacrificed after inhaling Halothane (Sigma, St Louis, MO). Brains were immediately removed, iced and cut into 300 μm slices by a Vibratome (Leica VP1000S, Leica Microsystems Inc.). Slices were then incubated in artificial CSF (in mM: 130 NaCl, 26 $NaHCO_3$, 3 KCl, 5 $MgCl_2$, 1.25 NaH_2PO_4, 1 $CaCl_2$, 10 glucose, pH 7.4, 300mOsm) for 1–6 hrs at room temperature (20–22°C) bubbling with 95% O_2, 5% CO_2. The PFC-containing slice was positioned in a perfusion chamber attached to the fixed stage of an upright microscope (Olympus, Center Valley, PA) and submerged in continuously flowing oxygenated artificial CSF. Bicuculline (20 μM) and CNQX (20 μM) were added in the recordings of N-methyl-D-aspartate receptor (NMDAR)-excitatory postsynaptic current (EPSC). Patch electrodes contained internal solution (in mM: 130 Cs-methanesulfonate, 10 CsCl, 4 NaCl, 10 HEPES (N-2-hydroxyethylpiperazine-N-2-ethane sulfonic acid), 1 $MgCl_2$, 5 EGTA (ethylene glycol tetraacetic acid), 2.2 QX-314, 12 phosphocreatine, 5 MgATP, 0.2 Na_2GTP, 0.1 leupeptin, pH 7.2–7.3 and 265-270mOsm). Cells were visualized with a 40× water-immersion lens and illuminated with near infrared light and the image was detected with an infrared-sensitive CCD camera. A Multiclamp 700A amplifier was used for these recordings. Tight seals (2-10GΩ) from visualized neurons were obtained by applying negative pressure. With additional suction, the membrane was disrupted into the whole-cell configuration. Evoked EPSC were generated with a pulse from a stimulation isolation unit controlled by a S48 pulse generator (Astro Med, West Warwick, RI). A bipolar stimulating electrode (FHC, Bowdoinham, ME) was placed ~100 μm from the neuron under recording. For NMDAR-EPSC, the cell (clamped at −70 mV) was depolarized to +60mV for 3 sec before stimulation to fully relieve the voltage-dependent Mg^{2+} block. To obtain the input/output responses, EPSC was elicited by a series of stimulation intensities (50–90 μA) with the same duration of pulses (0.6 ms).

Whole-cell NMDA-elicited currents in cultured neurons were recorded using standard voltage-clamp techniques (Yuen et al., 2011, 2012). The internal solution contained the

following (in mM): 180 N-methyl-D-glucamine, 4 $MgCl_2$, 40 HEPES, 0.5 BAPTA, 12 phosphocreatine, $3Na_2ATP$, and $0.5Na_2GTP$, with pH 7.2–7.3 and 265–270 mOsm. The external solution consisted of the following (in mM: 127 NaCl, 20 CsCl, 1 $CaCl_2$, 5 $BaCl_2$, 10 HEPES, 12 glucose, 0.02 glycine, and 0.001 tetrodotoxin, pH 7.4, and 300 mOsm). Recordings were obtained using Axopatch200B patch-clamp amplifier (Molecular Devices), controlled with a computer running Clampex 10.2 with a DigiData 1440A series interface (Molecular Devices). A tight seal (>2 GΩ) was obtained using negative pressure, with membrane disruption after additional suction. The cell membrane was held at −60 mV, and NMDAR-mediated current was elicited by bath application of NMDA (100 μM) for 2 sec every 30 sec.

Data analyses were performed with Clampfit (Axon instruments, Molecular Devices, Sunnyvale, CA, USA), Kaleidagraph (Albeck Software, Synergy Software, Reading, PA, USA) and GraphPad Prism 6 (GraphPad Software, Inc., La Jolla, CA).

Biochemical measurement of surface-expressed receptors

After treatment, viral infected PFC slices (300 μm) were incubated with ACSF containing 1 mg/ml sulfo-N-hydroxysuccinimide-LC-Biotin (Pierce, Rockford, IL) for 20 min on ice. The slices were then rinsed three times in TBS to quench the biotin reaction. PFC punches (diameter is 1.5 mm) with GFP signals were dissected out, followed by homogenization in 300 μl of modified radioimmunoprecipitation assay buffer (1% Triton X-100, 0.1% SDS, 0.5% deoxycholic acid, 50 mM $NaPO_4$, 150 mM NaCl, 2 mM EDTA, 50 mM NaF, 10 mM sodium pyrophosphate, 1 mM sodium orthovanadate, 1 mM PMSF, and 1 mg/ml leupeptin). For each sample, the total eight PFC punches from two mice were combined. The homogenates were centrifuged at 14,000 × g for 15 min at 4°C. 15 μg of protein were removed to measure total NR1. For surface protein, 150 μg of protein was incubated with 100 μl of 50% Neutravidin Agarose (Pierce) for 2 hr at 4°C, and bound proteins were resuspended in 25 μl of SDS sample buffer and boiled. Quantitative Western blots were performed on both total and biotinylated (surface) proteins using anti-NR1 (1:250, NeuroMab 75-272).

Behavioral tests

All experiments were performed between 1pm and 5pm under dim illumination. Behaviors were done by investigators blinded to treatment or genotype condition. Behavioral tests were performed at 3 days after the stereotaxic injection of hD4.x Sindbis virus.

Open field test—Animals were placed in an open-field (60 cm × 80 cm), and the amount of time the animal spent in the center (25 cm × 25 cm) was counted. A single mouse was placed into the center of open-field arena and their behavior was recorded over a 5-min session. Anxiety level were measured by the relative amount of exploration devoted to the center quadrants relative to those located adjacent to the walls of the arena. This was quantified by two indices: (i) time spent in the center quadrants and (ii) number of entries into the center quadrants. An entry into a given quadrant was only registered if all four paws were placed inside the quadrant. Open-field arena was carefully cleaned between tests to minimize odor cues.

Elevated plus maze—The maze was a plastic plus-shaped apparatus, and elevated at a height of 50cm. It consisted of two open arms (50×10 cm) and two enclosed arms (50×10×50 cm), all arms having an open roof. Each mouse was placed in the center of the maze facing one of the closed arms. Entries and the time spent in open or closed arms were recorded for 5 min. An entry was counted only if all four paws were inside the arm. Four parameters were measured during each 5-min rest: 1) time spent in the open arms; 2) time spent in the closed arms; 3) number of entries into the open arms; 4) number of crossing between the closed arms (Shah et al., 2004).

Locomotion Test—Animals were placed in a large cage devoid of any bedding materials for 5 minutes and the number of times crossing a midline was counted.

Statistics

All data are expressed as the mean ± SEM. Experiments with two groups were analyzed statistically using unpaired Student's t tests. Experiments with more than two groups were subjected to one-way ANOVA, followed by post hoc Tukey's tests.

RESULTS

Human D4 receptor binds to the SH3 domain of PSD-95 in a state-dependent manner

To understand the synaptic function of human D4 receptor variants, we first examined their interaction with SH3 domain-containing synaptic proteins. HEK293 cells were transfected with hD_4R variants with 0, 2, 4, or 7 proline-rich repeats (hD4.x) and PSD-95. As illustrated in Fig. 1A, hD4.2, hD4.4, and hD4.7 showed strong binding to full-length PSD-95 (PSD-95FL) or PSD-95 with the deleted guanylate kinase (GK) domain (PSD-95ΔGK), but not PSD-95 with the deleted SH3 domain (PSD-95ΔSH3), suggesting that the SH3 domain on PSD-95 is the D_4R binding site. Moreover, hD4.0, which does not contain the tandem repeats, showed no interaction with PSD-95, confirming that the proline-rich repeats on hD_4R are the PSD-95 binding site.

Next, we examined hD4R/PSD-95 interaction *in vivo*. HA-tagged hD4.x Sindbis virus was stereotaxically injected into the medial PFC region of $D_4R^{-/-}$ mice. The viral infected areas were dissected out for co-immunoprecipitation assays. As illustrated in Fig. 1B, hD4.4 and hD4.7 showed interactions with endogenous PSD-95, while hD4.7 bound to even more PSD-95 than hD4.4 (~80% more, n = 5). Interestingly, activation of hD4 receptors with the specific agonist PD168077 (20 μM, 10 min) led to a substantial reduction of their interaction with PSD-95 (hD4.4: ~70% reduction; hD4.7: ~85% reduction, n = 5). After washing off the agonist, the hD4.x/PSD-95 interaction restored. It suggests that hD4 receptors at the inactive state physically associate with PSD-95, whereas activation of hD4.x changes the receptor conformation, which disturbs its binding to PSD-95.

To find out whether there is a direct interaction between D4 and NMDA receptors, we transfected HEK293 cells with HA-tagged hD4.x and NR1 alone or NR1 plus NR2B constructs, and performed co-immunoprecipitation experiments. As shown in Fig. 1C, no NR1 signal was detected in hD4.x immunoprecipitates (detected with anti-HA), indicating that D4 receptors do not directly associate with NMDARs.

Activation of hD4.7 induces more suppression of NR1/PSD-95 binding and NMDAR surface expression

Our biochemical studies have for the first time revealed the binding of human D_4 receptors with the postsynaptic scaffolding protein PSD-95. PSD-95 binds to the C-terminus of NMDA receptor subunits via the PDZ domain (Kornau et al., 1995), controlling NMDAR internalization and NMDAR synaptic targeting (Roche et al., 2001; Wenthold et al., 2003; Prybylowski et al., 2005). Thus, D_4 receptors may regulate NMDA receptors via the common binding partner, PSD-95. To test this, we examined whether activation of human D_4R variants differentially affects NMDAR/PSD-95 interaction, therefore NMDAR trafficking.

$D_4R^{-/-}$ mice with PFC injection of hD4.x Sindbis virus was used to examine the impact of hD4 variants on NR1/PSD-95 interaction. As shown in Fig. 2A, application of PD168077 (20 μM, 10 min) caused a much more prominent reduction of NR1/PSD-95 complex in hD4.7-expressing neurons than hD4.4-expressing neurons (hD4.4: ~15% reduction; hD4.7: ~80% reduction, $n = 5$, $p < 0.01$, ANOVA).

The substantial disruption of NMDAR/PSD-95 interaction by hD4.7 activation suggests that hD4.7 may exert a big effect on NMDAR membrane trafficking. To test this, we used the surface biotinylation assays (Wang et al., 2003; Yuen et al., 2009; 2011; 2012) to examine the impact of hD4 variants on NMDAR surface expression in $D_4R^{-/-}$ mice with PFC injection of hD4.x Sindbis virus. As shown in Fig. 2B, the level of surface NMDAR NR1 subunit was significantly reduced by PD168077 (20 μM, 10 min) in hD4.7-expressing neurons than hD4.4-expressing neurons (hD4.4: <10% reduction, $n = 10$; hD4.7: ~50% reduction, $n = 11$, $p < 0.01$, ANOVA). It confirms that hD4.7 activation tends to induce a stronger loss of NMDARs from the cell membrane.

Activation of hD4.7 induces NMDAR hypofunction

Previous studies have found that NMDAR association with PSD-95 increases the number of functional channels at the cell surface and channel opening rate of NMDARs (Roche et al., 2001; Lin et al., 2004). Thus, the different effects of hD4.7 vs. hD4.4 activation on NMDAR/PSD-95 interaction raise the possibility that NMDAR function is differentially regulated by these human D_4R variants. To test this, we examined the impact of hD4.x on NMDAR-mediated channel currents and synaptic responses in PFC neurons.

First, primary neuronal cultures from PFC of $D_4R^{-/-}$ mice were infected with hD4.4 or hD4.7 virus, and whole-cell NMDAR-mediated currents were recorded. No significant difference was found on the baseline NMDAR current density (pA/pF) between D4R KO neurons, hD4.4-expressing neurons, and hD4.7-expressing neurons (D4R KO: 34.4 ± 4.2; hD4.4: 37.1 ± 3.6; hD4.7: 40.0 ± 4.5. $n = 10$ per group) (Fig. 3A). We then examined the effect of hD4.x on NMDAR currents in these neurons. As shown in Fig. 3B, application of PD168077 (20 μM) had little effect on the amplitude of NMDAR currents in D4R KO neurons (1.5% ± 0.6%, $n = 10$), and produced a modest reduction of NMDAR currents in hD4.4-expressing neurons (12.7% ± 1.4%, $n = 10$), but caused a much more prominent

reduction of NMDAR currents in hD4.7-expressing neurons (30.1% ± 2.3%, n = 9, $p < 0.01$, ANOVA, compared to hD4.4).

Next, $D_4R^{-/-}$ mice were stereotaxically injected with hD4.x Sindbis virus into the medial PFC region, and NMDAR-EPSC was recorded in slices. No significant difference was found on the baseline NMDAR-EPSC induced by a series of stimulus intensities in hD4.4- or hD4.7-expressing neurons (data not shown). However, application of PD168077 (20 μM) caused a significantly bigger reduction of NMDAR-EPSC amplitude in hD4.7-expressing neurons than hD4.4-expressing neurons (Fig. 3C, 3E, & 3F, hD4.7, 42% ± 4% reduction, n = 10; hD4.4, 22% ± 3% reduction, n = 10, $p < 0.05$, ANOVA). NMDAR-EPSC was stable in the absence of the D_4R agonist. PFC neurons expressing the GFP-conjugated hD4.4 or hD4.7 virus exhibited normal morphological structures (Fig. 3G). These data suggest that activation of hD4.7 induces prominent NMDAR hypofunction, probably due to its impairment of NMDAR/PSD-95 interaction.

Finally, we examined whether D-cycloserine, a partial agonist at the glycine-binding site of NMDARs, could rescue the NMDAR hypofunction induced by hD4.7 activation. D-cycloserine (20 mg/kg) was systemically administrated to hD4.7-expressing mice, followed by NMDAR-EPSC recordings in PFC slices. As shown in Fig. 3D, 3E & 3F, D-cycloserine enhanced baseline NMDAR-EPSC (44% ± 6% increase, n = 10), and prevented the over-suppression of NMDAR-EPSC by PD168077 in hD4.7-expressing neurons (n = 10, $p > 0.05$, ANOVA, compared to hD4.4).

The hD4.7-expressing mice exhibit ADHD-like behaviors, which can be ameliorated by D-cycloserine treatment

To understand the potential implication of hD4.7-induced NMDAR hypofunction, we examined behavioral alterations of hD4.7-expressing mice without or with D-cycloserine treatment. Two commonly used approach-avoidance conflict tasks, open-field and elevated plus maze (Dulawa et al., 1999; Chen et al., 2006), were used to examine the exploratory and novelty seeking behaviors in D4R KO mice with PFC expression of hD4.4 or hD4.7.

Comparing to WT or hD4.4-expressing mice, hD4.7-expressing mice exhibited significantly increased exploratory behaviors in the open-field test (Fig. 4A), as demonstrated by the increased time spent in the center compartment (WT: 9.3 ± 0.9 sec; hD4.4: 10.8 ± 1.0 sec; hD4.7: 22.7 ± 2.3 sec, n = 14–17 per group, $F_{4,79} = 19.4$, $p < 0.001$, one-way ANOVA), the increased number of entries into the center (WT: 5.1 ± 0.5 sec; hD4.4: 4.5 ± 0.3 sec; hD4.7: 6.8 ± 0.4 sec, n = 14–17 per group, $F_{4,79} = 6.6$, $p < 0.01$, one-way ANOVA), and the increased time in the center per entry (WT: 1.8 ± 0.1 sec; hD4.4: 2.4 ± 0.2 sec; hD4.7: 3.5 ± 0.4 sec, n = 14–17 per group, $F_{4,79} = 10.1$, $p < 0.01$, one-way ANOVA). The increased exploratory behaviors in hD4.7-expressing mice were not due to hyperactivity, as locomotion tests did not find significant differences among WT, hD4.4- or hD4.7-expressing mice (# midline crossing, WT: 23.4 ± 1.3; hD4.4: 21.2 ± 1.1; hD4.7: 21.6 ± 0.9, n = 17–19 per group, $F_{4,81} = 1.1$, $p > 0.05$, one-way ANOVA).

Next, hD4.7 mice were injected with D-cycloserine (20 mg/kg) at 30 mins before the open-field testing. As shown in Fig. 4A, the increased exploratory behaviors in hD4.7 mice were

ameliorated by D-cycloserine treatment, as demonstrated by the decreased time spent in the center compartment (hD4.7+saline: 24.2 ± 2.9 sec, hD4.7+cycloserine: 8.1 ± 1.0 sec, n = 14–17 per group; $p < 0.01$, one-way ANOVA), the decreased number of center entries (hD4.7+saline: 6.7 ± 0.6, hD4.7+cycloserine: 4.3 ± 0.5, n = 14–17 per group; $p < 0.05$, one-way ANOVA), and the decreased time in the center per entry (hD4.7+saline: 3.7 ± 0.4 sec, hD4.7+cycloserine: 2.0 ± 0.2 sec, n = 14–17 per group. $p < 0.01$, one-way ANOVA).

In the elevated plus maze test (Fig. 4B), hD4.7-expressing mice also exhibited significantly increased exploratory and risk taking behaviors, as demonstrated by the increased time spent in open arms (hD4.4: 6.2 ± 3.1 sec; hD4.7: 16.4 ± 3.2 sec, n = 11–17 per group, $F_{3,56} = 3.1$, $p < 0.05$, one-way ANOVA), and the increased number of entries into open arms (hD4.4: 1.3 ± 0.5; hD4.7: 2.8 ± 0.6, n = 11–17 per group, $F_{3,56} = 2.9$, $p < 0.05$, one-way ANOVA). D-cycloserine treatment reversed the exploratory behaviors in hD4.7 mice, as demonstrated by the decreased time spent in open arms (hD4.7+saline: 16.7 ± 3.1 sec, hD4.7+cycloserine: 8.0 ± 2.1 sec, n=11–17 per group, $p < 0.05$, one-way ANOVA), and the decreased number of entries into open arms (hD4.7+saline: 2.9 ± 0.7, hD4.7+cycloserine: 1.3 ± 0.3, n =11–17 per group, $p < 0.05$, one-way ANOVA).

Discussion

In this study, we have provided physiological, biochemical and behavioral evidence to demonstrate the molecular mechanism and functional significance of human D4R exon III polymorphism, which may contribute to its role in executive control deficiencies of ADHD (LaHoste et al., 1996; Swanson et al., 1998; Talkowski et al., 2008; Gizer et al., 2009; Barnes et al., 2011) and personality trait of novelty seeking and risk taking (Ebstein et al., 1996; Vaughn et al., 2009; Eisenegger et al., 2010).

Little is known about the mechanisms underlying the functional differences of hD_4R variants (Gonzalez et al., 2012). Pharmacological profiles or the abilities to block cAMP production are similar among hD4.x isoforms (Asghari et al., 1995; Jovanovic et al., 1999). The additional 2–11 proline-rich repeats located in the third intracellular loop of human D_4R, a unique primate-specific feature of the receptor (Wang et al., 2004), allows more complex simultaneous interactions with other proteins containing the SH3 domain. Using transfected cell lines, we have demonstrated the direct interaction of the proline-rich repeats of human D4Rs with the SH3 domain of PSD-95, a scaffolding protein for NMDARs (Fig. 1A). This hD4R/PSD-95 interaction also occurs *in vivo*, but it is reduced by the presence of a D4R agonist, suggesting a dynamic and state-dependent nature of the protein complex (Fig. 1B).

Since PSD-95 plays a key role in regulating NMDAR surface expression (Roche et al., 2001; Wenthold et al., 2003; Prybylowski et al., 2005), the binding of hD4R to PSD-95 raises the possibility that it might affect the association of NMDARs with PSD-95 and the membrane stability of NMDARs. Indeed, we have found that activation of hD4.7, but not hD4.4, leads to a dramatic loss of NMDAR/PSD-95 complex (Fig. 2A), which results in a significant reduction of the level of surface NMDARs (Fig. 2B).

Our previous electrophysiological studies in rodents have shown that D4R activation in PFC pyramidal neurons reduces NMDAR currents (Wang et al., 2003). Similar effects on NMDAR-mediated ionic or synaptic currents have been found with virally expressed hD4.4, however, activation of hD4.7 induces a significantly bigger reduction of NMDAR currents (Fig. 3B, C), which may be caused by the hD4.7-induced loss of NMDAR/PSD-95 complex and surface NMDARs (Fig. 2).

The over-suppression of NMDARs by hD4.7 suggests that it may induce PFC hypoactivity. Consistently, our recent study has found that the synchronous excitatory network bursts originating from the large scale correlated activity of interconnected neurons, which require NMDA receptors, are more prominently suppressed by hD4.7 than hD4.4 in PFC pyramidal neurons (Zhong et al., 2015). Synchronized network activity in cortex has been suggested to cooperatively support temporal representation and long-term consolidation of information (Buzsáki & Draguhn, 2004), which controls selective attention (Womelsdorf et al., 2007; Womelsdorf and Fries, 2007; Buschman and Miller, 2007; Miller and Buschman, 2013). The hD4.7-induced NMDAR hypofunction and aberrant synchronous network activity (Zhong et al., 2015) may explain the significant frontal hypoactivity detected in ADHD patients (Dickstein et al., 2006; Fernández et al., 2009).

To directly assess the potential implication of the dysregulation of NMDARs by ADHD-linked hD4.7 variant, we have examined novelty seeking behaviors. Novel stimuli, such as unfamiliar environments, are theorized to create conflict in rodents by concurrently evoking both approach and avoidance behaviors (Montgomery, 1955). Approach behavior or “exploration” reflects an animal’s tendency to explore novel stimuli or environments, whereas avoidance behavior or “anxiety-related behavior” is thought to reflect an animal’s fear of novelty (Dulawa et al., 1999). By using two approach-avoidance conflict tasks, open-field and elevated plus maze, we have found that D4R knockout mice with hD4.7 expression in PFC exhibit significantly increased exploratory behaviors than those with hD4.4 expression (Fig. 4). These abnormalities are consistent with the idea that hD4.7 may play important roles in human behaviors related to novelty seeking, such as drug abuse (Kotler et al., 1997) and gambling (Comings et al., 1999; Eisenegger et al., 2010), and in the higher risk taking behaviors of ADHD patients (LaHoste et al., 1996; Kaye et al., 2014).

To counteract the physiological and behavioral abnormalities induced by hD4.7 activation, we have administered D-cycloserine, a partial agonist at the glycine-binding site of NMDARs. D-cycloserine enhances basal NMDAR-mediated synaptic current in hD4.7-expressing neurons, and prevents NMDAR hypofunction induced by hD4.7 activation (Fig. 3D–F). In parallel, D-cycloserine treatment has ameliorated the higher novelty seeking behaviors in hD4.7-expressing mice (Fig. 4). It suggests that enhancing NMDAR function with D-cycloserine is a potential therapeutic avenue for normalizing behavioral deficits in ADHD and related mental disorders, such as autism (Blundell et al., 2010; Won et al., 2012). Our results are based on virally expressed human D4 receptor variants, which are likely to have a higher expression level than endogenously expressed D4 receptors. Thus, caution is needed regarding the therapeutic use of D-cycloserine.

Acknowledgments

We would like to thank Xiaoqing Chen for her excellent technical support. This work was supported by NIH grants (DA037618, MH108842) and a Nancy Lurie Marks Family Foundation grant to ZY, and NSFC grant (31271124) and Guangdong Natural Science Foundation grant (S2013010016062) to WL.

References

Altink ME, Rommelse NN, Slaats-Willemse DI, Vasquez AA, Franke B, Buschgens CJ, Fliers EA, Faraone SV, Sergeant JA, Oosterlaan J, Buitelaar JK. The dopamine receptor D4 7-repeat allele influences neurocognitive functioning, but this effect is moderated by age and ADHD status: an exploratory study. World J Biol Psychiatry. 2012; 13:293–305. [PubMed: 22111665]

Asghari V, Sanyal S, Buchwaldt S, Paterson A, Jovanovic V, Van Tol HH. Modulation of intracellular cyclic AMP levels by different human dopamine D4 receptor variants. J Neurochem. 1995; 65:1157–1165. [PubMed: 7643093]

Avale ME, Falzone TL, Gelman DM, Low MJ, Grandy DK, Rubinstein M. The dopamine D4 receptor is essential for hyperactivity and impaired behavioral inhibition in a mouse model of attention deficit/hyperactivity disorder. Molecular psychiatry. 2004; 9:718–726. [PubMed: 14699433]

Barnes JJ, Dean AJ, Nandam LS, O'Connell RG, Bellgrove MA. The molecular genetics of executive function: role of monoamine system genes. Biol Psychiatry. 2011; 69:e127–43. [PubMed: 21397212]

Batty MJ, Palaniyappan L, Scerif G, Groom MJ, Liddle EB, Liddle PF, Hollis C. Morphological abnormalities in prefrontal surface area and thalamic volume in attention deficit/hyperactivity disorder. Psychiatry Res. 2015; 233:225–32. [PubMed: 26190555]

Benjamin J, Li L, Patterson C, Greenberg BD, Murphy DL, Hamer DH. Population and familial association between the D4 dopamine receptor gene and measures of Novelty Seeking. Nat Genet. 1996; 12:81–84. [PubMed: 8528258]

Berry D, Deater-Deckard K, McCartney K, Wang Z, Petrill SA. Gene-environment interaction between dopamine receptor D4 7-repeat polymorphism and early maternal sensitivity predicts inattention trajectories across middle childhood. Dev Psychopathol. 2013; 25:291–306. [PubMed: 23627945]

Blundell J, Blaiss CA, Etherton MR, Espinosa F, Tabuchi K, Walz C, Bolliger MF, Sudhof TC, Powell CM. Neuroligin-1 deletion results in impaired spatial memory and increased repetitive behavior. The Journal of neuroscience. 2010; 30:2115–2129. [PubMed: 20147539]

Bobb AJ, Castellanos FX, Addington AM, Rapoport JL. Molecular genetic studies of ADHD: 1991 to 2004. Am J Med Genet B Neuropsychiatr Genet. 2005; 132B(1):109–25. [PubMed: 15700344]

Brozoski TJ, Brown RM, Rosvold HE, Goldman PS. Cognitive deficit caused by regional depletion of dopamine in prefrontal cortex of rhesus monkey. Science. 1979; 205:929–932. [PubMed: 112679]

Buschman TJ, Miller EK. Top-down versus bottom-up control of attention in the prefrontal and posterior parietal cortices. Science. 2007; 315:1860–2. [PubMed: 17395832]

Buzsáki G, Draguhn A. Neuronal oscillations in cortical networks. Science. 2004; 304:1926–9. [PubMed: 15218136]

Chang FM, Kidd JR, Livak KJ, Pakstis AJ, Kidd KK. The worldwide distribution of allele frequencies at the human dopamine D4 receptor locus. Hum Gene. 1996; 98:91–101.

Chang JP, Lane HY, Tsai GE. Attention deficit hyperactivity disorder and N-methyl-D-aspartate (NMDA) dysregulation. Curr Pharm Des. 2014; 20:5180–5185. [PubMed: 24410567]

Cheng J, Xiong Z, Duffney LJ, Wei J, Liu A, Liu S, Chen GJ, Yan Z. Methylphenidate Exerts Dose-Dependent Effects on Glutamate Receptors and Behaviors. Biological psychiatry. 2014; 76:953–62. [PubMed: 24832867]

Comings DE, Gonzalez N, Wu S, Gade R, Muhleman D, Saucier G, Johnson P, Verde R, Rosenthal RJ, Lesieur HR, Rugle LJ, Miller WB, MacMurray JP. Studies of the 48 bp repeat polymorphism of the DRD4 gene in impulsive, compulsive, addictive behaviors: Tourette syndrome, ADHD, pathological gambling, and substance abuse. Am J Med Genet. 1999; 88:358–368. [PubMed: 10402503]

Dickstein SG, Bannon K, Castellanos FX, Milham MP. The neural correlates of attention deficit hyperactivity disorder: an ALE meta-analysis. J Child Psychol Psychiatry. 2006; 47:1051–62. [PubMed: 17073984]

Dorval KM, Wigg KG, Crosbie J, Tannock R, Kennedy JL, Ickowicz A, Pathare T, Malone M, Schachar R, Barr CL. Association of the glutamate receptor subunit gene GRIN2B with attention-deficit/hyperactivity disorder. Genes, brain, and behavior. 2007; 6:444–452.

Duffney LJ, Zhong P, Wei J, Matas E, Cheng J, Qin L, Ma K, Dietz DM, Kajiwara Y, Buxbaum JD, Yan Z. Autism-like Deficits in Shank3-Deficient Mice Are Rescued by Targeting Actin Regulators. Cell reports. 2015; 11:1400–1413. [PubMed: 26027926]

Dulawa SC, Grandy DK, Low MJ, Paulus MP, Geyer MA. Dopamine D4 receptor-knockout mice exhibit reduced exploration of novel stimuli. J Neurosci. 1999; 19:9550–9556. [PubMed: 10531457]

Ebstein RP, Novick O, Umansky R, Priel B, Osher Y, Blaine D, Bennett ER, Nemanov L, Katz M, Belmaker RH. Dopamine D4 receptor (D4DR) exon III polymorphism associated with the human personality trait of Novelty Seeking. Nat Genet. 1996; 12:78–80. [PubMed: 8528256]

Eisenegger C, Knoch D, Ebstein RP, Gianotti LR, Sandor PS, Fehr E. Dopamine receptor D4 polymorphism predicts the effect of L-DOPA on gambling behavior. Biological psychiatry. 2010; 67:702–706. [PubMed: 19914604]

Fernández A, Quintero J, Hornero R, Zuluaga P, Navas M, Gómez C, Escudero J, García-Campos N, Biederman J, Ortiz T. Complexity analysis of spontaneous brain activity in attention-deficit/hyperactivity disorder: diagnostic implications. Biol Psychiatry. 2009; 65:571–7. [PubMed: 19103438]

Gizer IR, Ficks C, Waldman ID. Candidate gene studies of ADHD: a meta-analytic review. Hum Genet. 2009; 126(1):51–90. [PubMed: 19506906]

Goldman-Rakic PS. Cellular basis of working memory. Neuron. 1995; 14:477–85. [PubMed: 7695894]

Gonzalez S, Rangel-Barajas C, Peper M, Lorenzo R, Moreno E, Ciruela F, Borycz J, Ortiz J, Lluis C, Franco R, McCormick PJ, Volkow ND, Rubinstein M, Floran B, Ferre S. Dopamine D4 receptor, but not the ADHD-associated D4.7 variant, forms functional heteromers with the dopamine D2S receptor in the brain. Molecular psychiatry. 2012; 17:650–662. [PubMed: 21844870]

Grady DL, Chi HC, Ding YC, Smith M, Wang E, Schuck S, Flodman P, Spence MA, Swanson JM, Moyzis RK. High prevalence of rare dopamine receptor D4 alleles in children diagnosed with attention-deficit hyperactivity disorder. Mol psychiatry. 2003; 8:536–545. [PubMed: 12808433]

Hawi Z, Cummins TD, Tong J, Johnson B, Lau R, Samarrai W, Bellgrove MA. The molecular genetic architecture of attention deficit hyperactivity disorder. Mol Psychiatry. 2015; 20:289–97. [PubMed: 25600112]

Jensen V, Rinholm JE, Johansen TJ, Medin T, Storm-Mathisen J, Sagvolden T, Hvalby O, Bergersen LH. N-methyl-D-aspartate receptor subunit dysfunction at hippocampal glutamatergic synapses in an animal model of attention-deficit/hyperactivity disorder. Neuroscience. 2009; 158:353–364. [PubMed: 18571865]

Jo J, Son GH, Winters BL, Kim MJ, Whitcomb DJ, Dickinson BA, Lee YB, Futai K, Amici M, Sheng M, Collingridge GL, Cho K. Muscarinic receptors induce LTD of NMDAR EPSCs via a mechanism involving hippocalcin, AP2 and PSD-95. Nat Neurosci. 2010; 13:1216–24. [PubMed: 20852624]

Jovanovic V, Guan HC, Van Tol HH. Comparative pharmacological and functional analysis of the human dopamine D4.2 and D4.10 receptor variants. Pharmacogenetics. 1999; 9:561–8. [PubMed: 10591536]

Kaye S, Gilsenan J, Young JT, Carruthers S, Allsop S, Degenhardt L, van de Glind G, van den Brink W. Risk behaviours among substance use disorder treatment seekers with and without adult ADHD symptoms. Drug Alcohol Depend. 2014; 144:70–77. [PubMed: 25193717]

Kornau HC, Schenker LT, Kennedy MB, Seeburg PH. Domain interaction between NMDA receptor subunits and the postsynaptic density protein PSD-95. Science. 1995; 269:1737–1740. [PubMed: 7569905]

Kotler M, Cohen H, Segman R, Gritsenko I, Nemanov L, Lerer B, Kramer I, Zer-Zion M, Kletz I, Ebstein RP. Excess dopamine D4 receptor (D4DR) exon III seven repeat allele in opioid-dependent subjects. Molecular psychiatry. 1997; 2:251–254. [PubMed: 9152990]

LaHoste GJ, Swanson JM, Wigal SB, Glabe C, Wigal T, King N, Kennedy JL. Dopamine D4 receptor gene polymorphism is associated with attention deficit hyperactivity disorder. Molecular psychiatry. 1996; 1:121–124. [PubMed: 9118321]

Li T, Chen CK, Hu X, Ball D, Lin SK, Chen W, Sham PC, Loh el-W, Murray RM, Collier DA. Association analysis of the DRD4 and COMT genes in methamphetamine abuse. Am J Med Genet B Neuropsychiatr Genet. 2004; 129B:120–4. [PubMed: 15274053]

Lin Y, Skeberdis VA, Francesconi A, Bennett MV, Zukin RS. Postsynaptic density protein-95 regulates NMDA channel gating and surface expression. The Journal of neuroscience : the official journal of the Society for Neuroscience. 2004; 24:10138–10148. [PubMed: 15537884]

Lisman JE, Fellous JM, Wang XJ. A role for NMDA-receptor channels in working memory. Nat Neurosci. 1998; 1:273–5. [PubMed: 10195158]

Miller EK, Buschman TJ. Cortical circuits for the control of attention. Curr Opin Neurobiol. 2013; 23:216–22. [PubMed: 23265963]

Montgomery KC. The relation between fear induced by novel stimulation and exploratory behavior. J Comp Physiol Psychol. 1955; 48:254–260. [PubMed: 13252152]

Mrzljak L, Bergson C, Pappy M, Huff R, Levenson R, Goldman-Rakic PS. Localization of dopamine D4 receptors in GABAergic neurons of the primate brain. Nature. 1996; 381:245–248. [PubMed: 8622768]

Popoli M, Yan Z, McEwen BS, Sanacora G. The stressed synapse: the impact of stress and glucocorticoids on glutamate transmission. Nat Rev Neurosci. 2011; 13:22–37. [PubMed: 22127301]

Prybylowski K, Chang K, Sans N, Kan L, Vicini S, Wenthold RJ. The synaptic localization of NR2B-containing NMDA receptors is controlled by interactions with PDZ proteins and AP-2. Neuron. 2005; 47:845–857. [PubMed: 16157279]

Reiner I, Spangler G. Dopamine D4 receptor exon III polymorphism, adverse life events and personality traits in a nonclinical German adult sample. Neuropsychobiology. 2011; 63:52–58. [PubMed: 21063133]

Roche KW, Standley S, McCallum J, Dune Ly C, Ehlers MD, Wenthold RJ. Molecular determinants of NMDA receptor internalization. Nature neuroscience. 2001; 4:794–802. [PubMed: 11477425]

Rondou P, Haegeman G, Vanhoenacker P, Van Craenenbroeck K. BTB Protein KLHL12 targets the dopamine D4 receptor for ubiquitination by a Cul3-based E3 ligase. J Biol Chem. 2008; 283:11083–96. [PubMed: 18303015]

Rubinstein M, Cepeda C, Hurst RS, Flores-Hernandez J, Ariano MA, Falzone TL, Kozell LB, Meshul CK, Bunzow JR, Low MJ, Levine MS, Grandy DK. Dopamine D4 receptor-deficient mice display cortical hyperexcitability. J Neurosci. 2001; 21:3756–3763. [PubMed: 11356863]

Rubinstein M, Phillips TJ, Bunzow JR, Falzone TL, Dziewczapolski G, Zhang G, Fang Y, Larson JL, McDougall JA, Chester JA, Saez C, Pugsley TA, Gershanik O, Low MJ, Grandy DK. Mice lacking dopamine D4 receptors are supersensitive to ethanol, cocaine, and methamphetamine. Cell. 1997; 90:991–1001. [PubMed: 9323127]

Shah AA, Sjovold T, Treit D. Selective antagonism of medial prefrontal cortex D4 receptors decreases fear-related behaviour in rats. Eur J Neurosci. 2004; 19:3393–3397. [PubMed: 15217397]

Swanson JM, Kinsbourne M, Nigg J, Lanphear B, Stefanatos GA, Volkow N, Taylor E, Casey BJ, Castellanos FX, Wadhwa PD. Etiologic subtypes of attention-deficit/hyperactivity disorder: brain imaging, molecular genetic and environmental factors and the dopamine hypothesis. Neuropsychol Rev. 2007; 17:39–59. [PubMed: 17318414]

Swanson JM, Sunohara GA, Kennedy JL, et al. Association of the dopamine receptor D4 (DRD4) gene with a refined phenotype of attention deficit hyperactivity disorder (ADHD): a family-based approach. Mol Psychiatry. 1998; 3:38–41. [PubMed: 9491811]

Talkowski ME, Kirov G, Bamne M, Georgieva L, Torres G, Mansour H, Chowdari KV, Milanova V, Wood J, McClain L, Prasad K, Shirts B, Zhang J, O'Donovan MC, Owen MJ, Devlin B,

Nimgaonkar VL. A network of dopaminergic gene variations implicated as risk factors for schizophrenia. Hum Mol Genet. 2008; 17:747–758. [PubMed: 18045777]

Thapar A, Cooper M. Attention deficit hyperactivity disorder. Lancet. 2015 Sep 16.

Trejo S, Toscano-Flores JJ, Matute E, Ramirez-Duenas Mde L. Hardy-Weinberg equilibrium analysis of the 48 bp VNTR in the III exon of the DRD4 gene in a sample of parents of ADHD cases. The application of clinical genetics. 2015; 8:133–136. [PubMed: 26082657]

Van Tol HH, Wu CM, Guan HC, Ohara K, Bunzow JR, Civelli O, Kennedy J, Seeman P, Niznik HB, Jovanovic V. Multiple dopamine D4 receptor variants in the human population. Nature. 1992; 358:149–152. [PubMed: 1319557]

Vaughn MG, Beaver KM, DeLisi M, Howard MO, Perron BE. Dopamine D4 receptor gene exon III polymorphism associated with binge drinking attitudinal phenotype. Alcohol. 2009; 43:179–184. [PubMed: 19393859]

Wang E, Ding YC, Flodman P, Kidd JR, Kidd KK, Grady DL, et al. The genetic architecture of selection at the human dopamine receptor D4 (DRD4) gene locus. Am J Hum Genet. 2004; 74:931–944. [PubMed: 15077199]

Wang X, Gu Z, Zhong P, Chen G, Feng J, Yan Z. Aberrant regulation of NMDA receptors by dopamine D4 signaling in rats after phencyclidine exposure. Molecular and cellular neurosciences. 2006; 31:15–25. [PubMed: 16198123]

Wang X, Zhong P, Gu Z, Yan Z. Regulation of NMDA receptors by dopamine D4 signaling in prefrontal cortex. J Neurosci. 2003; 23:9852–9861. [PubMed: 14586014]

Wedzony K, Chocyk A, Mackowiak M, Fijal K, Czyrak A. Cortical localization of dopamine D4 receptors in the rat brain–immunocytochemical study. J Physiol Pharmacol. 2000; 51:205–21. [PubMed: 10898094]

Wenthold RJ, Prybylowski K, Standley S, Sans N, Petralia RS. Trafficking of NMDA receptors. Annu Rev Pharmacol Toxicol. 2003; 43:335–358. [PubMed: 12540744]

Womelsdorf T, Fries P. The role of neuronal synchronization in selective attention. Curr Opin Neurobiol. 2007; 17:154–60. [PubMed: 17306527]

Womelsdorf T, Schoffelen JM, Oostenveld R, Singer W, Desimone R, Engel AK, Fries P. Modulation of neuronal interactions through neuronal synchronization. Science. 2007; 316:1609–12. [PubMed: 17569862]

Won H, Lee HR, Gee HY, Mah W, Kim JI, Lee J, Ha S, Chung C, Jung ES, Cho YS, Park SG, Lee JS, Lee K, Kim D, Bae YC, Kaang BK, Lee MG, Kim E. Autistic-like social behaviour in Shank2-mutant mice improved by restoring NMDA receptor function. Nature. 2012; 486:261–265. [PubMed: 22699620]

Yamaguchi Y, Lee YA, Goto Y. Dopamine in socioecological and evolutionary perspectives: implications for psychiatric disorders. Front Neurosci. 2015; 9:219. [PubMed: 26136653]

Yuen EY, Liu W, Karatsoreos IN, Feng J, McEwen BS, Yan Z. Acute stress enhances glutamatergic transmission in prefrontal cortex and facilitates working memory. Proc Natl Acad Sci U S A. 2009; 106:14075–9. [PubMed: 19666502]

Yuen EY, Wei J, Liu W, Zhong P, Li X, Yan Z. Repeated stress causes cognitive impairment by suppressing glutamate receptor expression and function in prefrontal cortex. Neuron. 2012; 73:962–977. [PubMed: 22405206]

Yuen EY, Liu W, Karatsoreos IN, Ren Y, Feng J, McEwen BS, Yan Z. Mechanisms for acute stress-induced enhancement of glutamatergic transmission and working memory. Molecular psychiatry. 2011; 16:156–170. [PubMed: 20458323]

Zhong P, Liu W, Yan Z. Aberrant regulation of synchronous network activity by the ADHD-associated human dopamine D4 receptor variant D4.7 in prefrontal cortex. J Physiol. 2016; 594:135–47. [PubMed: 26541360]

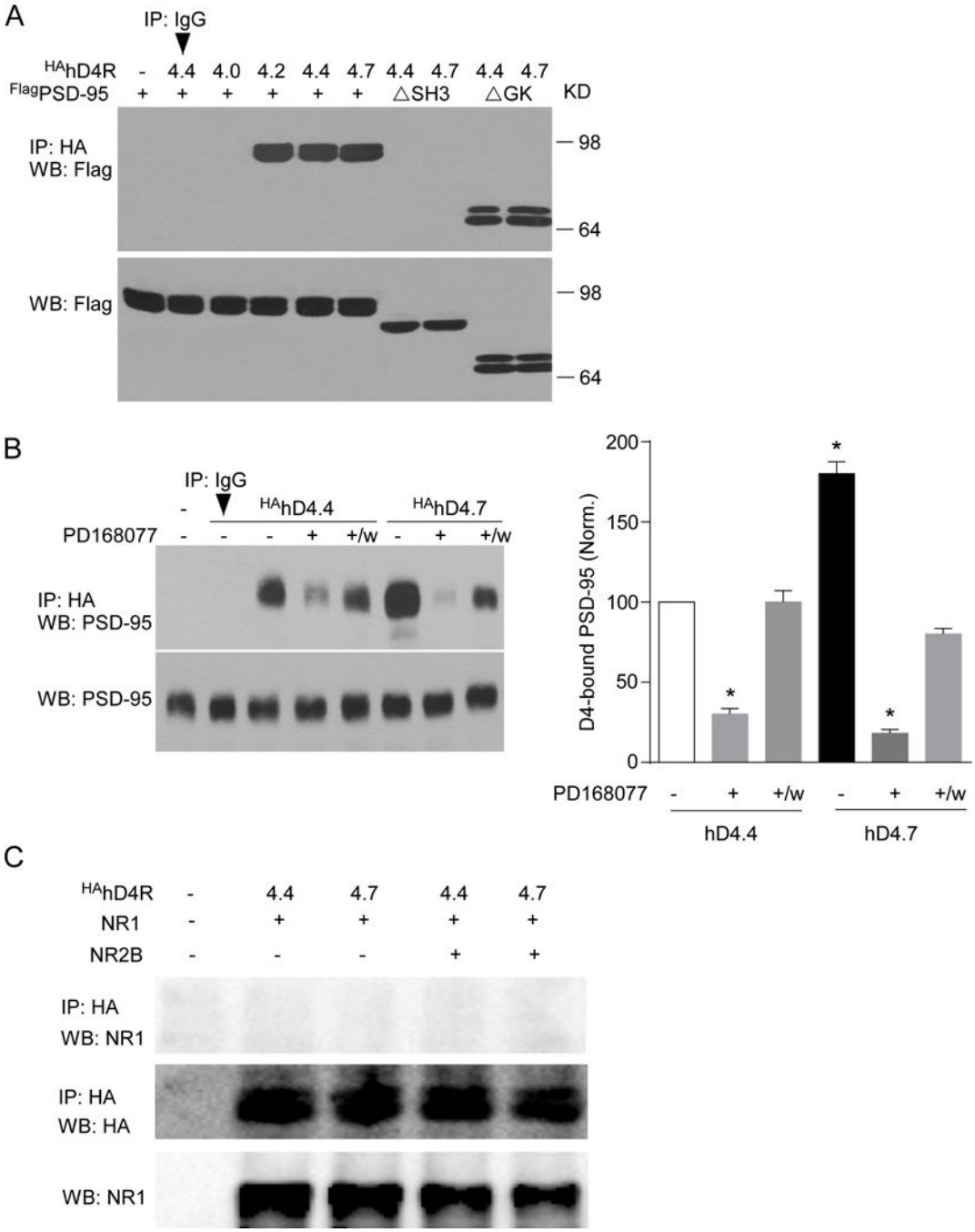

Fig. 1. The human D4 receptor dynamically binds to PSD-95 at the SH3 domain

(A) HEK293 cells were transfected with HA-tagged hD4.x (hD4.0, hD4.2, hD4.4, hD4.7) and Flag-tagged PSD-95 constructs (PSD-95FL, PSD-95ΔSH3, PSD-95ΔGK), and co-immunoprecipitation experiments were conducted to detect the hD4.x/PSD-95 interaction. The expression of PSD-95 constructs was detected with straight WB. **(B)** Co-immunoprecipitation blots and quantification showing the binding of virally expressed HA-tagged hD4.x with endogenous PSD-95 in D4R KO mice in the absence (−) or presence of PD168077 application (+), or at 30 min after washing off PD168077 (+/w) in PFC slices. *:

$p < 0.05$, **, $p < 0.01$, ANOVA, compared to hD4.4 (−). **(C)** HEK293 cells were transfected with HA-tagged hD4.x (hD4.4, hD4.7), NR1 and NR2B constructs, and co-immunoprecipitation experiments were conducted to detect the hD4.x/NR1 interaction. The expression of NR1 was detected with straight WB.

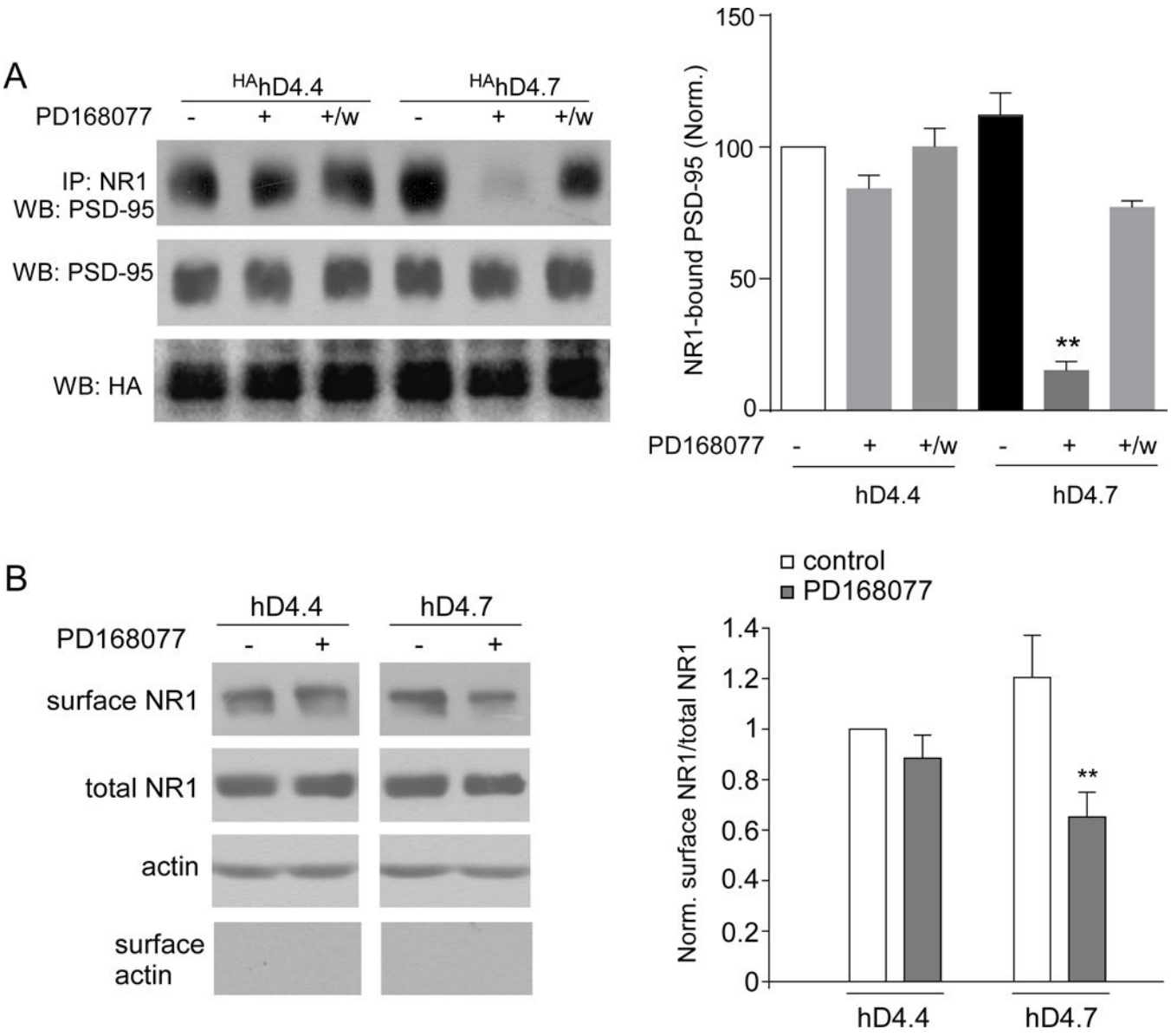

Fig. 2. Activation of hD4.7 disrupts NMDAR/PSD-95 interaction and reduces the surface expression of NMDA receptors

(A) Co-immunoprecipitation blots and quantification showing the binding of endogenous NR1 with PSD-95 in the absence (−) or presence of PD168077 application (+), or at 30 min after washing off PD168077 (+/w) in PFC slices from D4R KO mice with viral infection of hD4.4 vs. hD4.7. The Western blots of PSD-95 or HA-tagged hD4.x (~55 KDa) are also shown. **: $p < 0.01$, ANOVA, compared to hD4.4 (−). **(B)** Immunoblots and quantification analysis of surface and total NMDAR NR1 subunits showing the effect of PD168077 in PFC slices from D4R KO mice with viral infection of hD4.4 vs. hD4.7. **: $p < 0.01$, ANOVA, compared to hD4.4 (control).

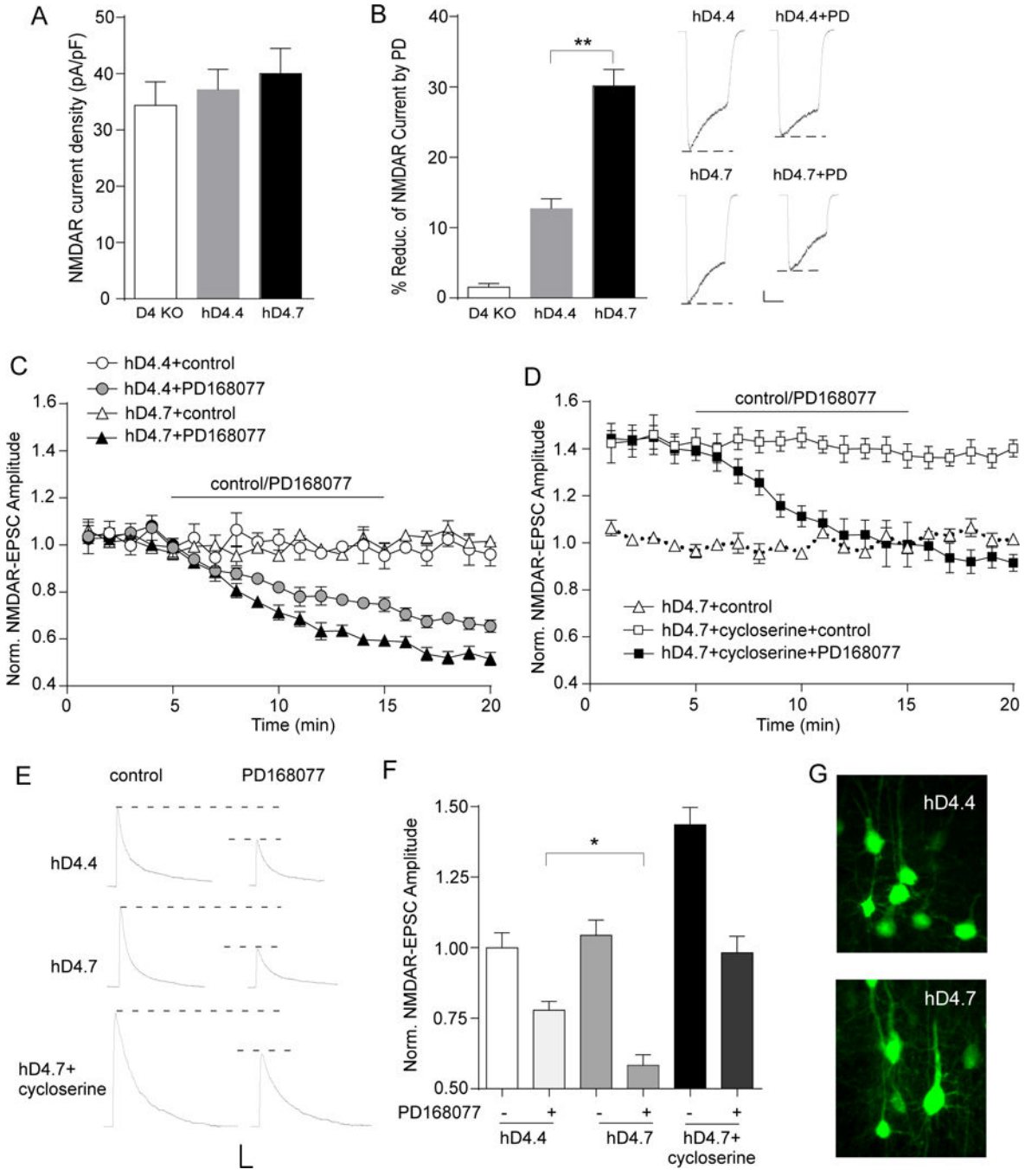

Fig. 3. NMDAR-mediated currents are strongly suppressed by activation of hD4.7, which is reversed by D-cycloserine

(A) Bar graphs showing the NMDAR current density in cortical cultures from D4R KO mice without or with the infection of hD4.4 vs. hD4.7 virus. **(B)** Bar graphs showing the percent reduction of NMDAR currents by PD168077 in cortical cultures from D4R KO mice without or with the infection of hD4.4 vs. hD4.7 virus. Inset, Representative current traces. Scale bars: 100 pA, 1 sec. **: $p < 0.01$, ANOVA, hD4.4 vs. hD4.7. **(C, D)** Plots of normalized NMDAR-EPSC showing the effect of PD168077 in representative PFC

pyramidal neurons from hD4.4- or hD4.7-expressing mice without or with D-cycloserine (20 mg/kg) treatment. **(E)** Representative EPSC traces. Scale bars: 50 pA, 100 ms. **(F)** Bar graphs showing the normalized NMDAR-EPSC amplitude before and after PD168077 application in different groups of neurons. *: $p < 0.05$, ANOVA, hD4.4 vs. hD4.7 in the presence of PD168077. **(G)** Confocal images of PFC neurons from D4R KO mice with the stereotaxic injection of GFP-tagged hD4.4 or hD4.7.

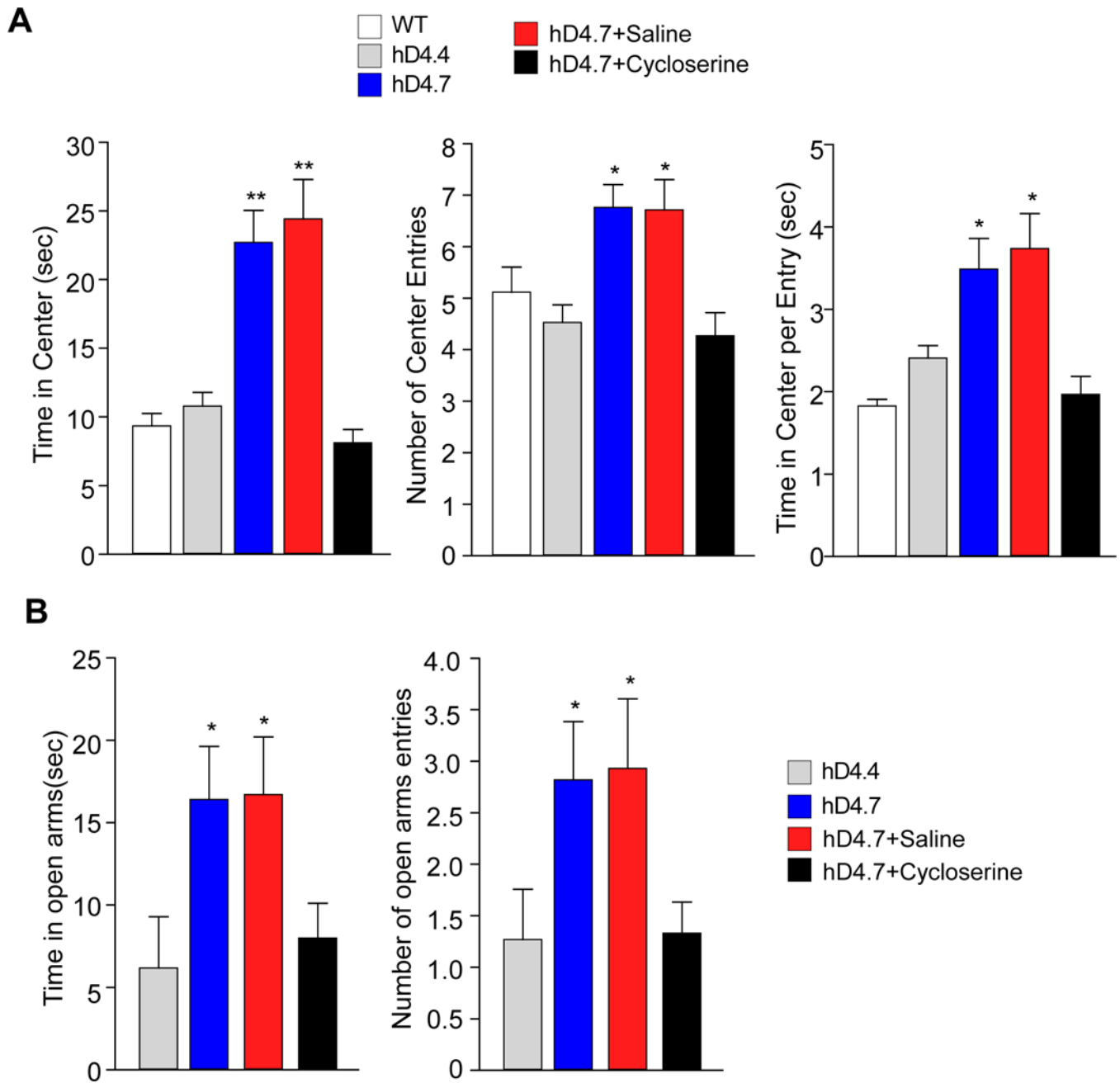

Fig. 4. The hD4.7-expressing mice exhibit increased exploratory and risk taking behaviors, which is reversed by D-cycloserine treatment

(A) Bar graphs showing the open-field test results of different groups of animals, including the time spent in the center, the number of entries into the center, and the time spent in the center per entry. *: $p < 0.05$, **: $p < 0.01$, ANOVA, compared to hD4.4. **(B)** Bar graphs showing the elevated plus maze test results of different groups of animals, including the time spent in the open arm and number of open arm entries. WT: wild-type, hD4.4: D4R KO mice with PFC injection of hD4.4 virus, hD4.7: D4R KO mice with PFC injection of hD4.7

virus, hD4.7+saline: hD4.7 mice treated with saline, hD4.7+cycloserine: hD4.7 mice treated with D-cycloserine. *: $p < 0.05$, ANOVA, compared to hD4.4.